Forest Ecology and Management 256 (2008) 99–105

Contents lists available at ScienceDirect

Forest Ecology and Management

journal homepage: www.elsevier.com/locate/foreco

Quantifying local factors in medium-frequency trends of tree ring records: Case study in Canadian boreal forests

Takeshi Ise *, Paul R. Moorcroft

Department of Organismic and Evolutionary Biology, Harvard University, Cambridge, MA 02138, USA

ARTICLE INFO

Article history:
Received 17 January 2008
Received in revised form 31 March 2008
Accepted 1 April 2008

Keywords:
Dendrochronology
Black spruce (*Picea mariana*)
Boreal forest
Stand dynamics
Dendroecology

ABSTRACT

Growth rings of a tree are simultaneously affected by various environmental constraints, including regional factors such as climate fluctuations and also local, gap-scale dynamics such as competition and stochastic mortality of neighbor trees. Although these local effects are often discarded by dendroclimatologists as random variation, the dendroecological trends may provide valuable information on past forest dynamics. Since dendroecological trends arising from local stand dynamics often have medium-term frequencies with persistence of several years to a few decades, it is usually difficult to separate local, gap-scale forcings from regional, medium-frequency forcings such as El Niño Southern Oscillation or North Atlantic Oscillation. Moreover, conventional dendroecological practices have failed to analyze the continuously changing medium frequency trends. In this study, a continuous index of medium-frequency dendrochronological trends was developed, by generalizing previous analytical methods that evaluate relative changes using moving averages. This method was then tested against a tree ring dataset from a site with a known history of release and suppression due to a hurricane disturbance. To quantify the effects of local gap dynamics against the regional, often climatic effects, increments cores of black spruce (*Picea mariana*) were sampled from boreal forests in Saskatchewan, Canada, using a stratified sampling design. Assuming that regional forcings affect trees in the given stand homogeneously, the relative effect of stochastic heterogeneity within stand was quantified. The results closely agreed with conventional dendrochronological observations. In closed-canopy stands, stochastic local effects explained 12.9–35.4% of the variation in tree ring widths, because interactions between neighbor trees were likely to be intense. In open-canopy stands, on the other hand, the proportion of explained variance was 1.4–10.2%, reflecting the less-intense local tree interactions in low-density stands. These advancements in statistical analysis and study design will help ecologists and paleoclimatologists to objectively evaluate the effects of climate fluctuations, relative to the effects of local, ecological interactions. Moreover, forest managers can apply concepts of filtering medium-frequency trends to assess release and suppression caused by forest management practices, such as selective cutting and forest thinning.

1. Introduction

Well-prepared dendrochronological data provide reliable long-term information on past environmental conditions (Fritts and Swetnam, 1989; Tessier et al., 1997). For example, dendroclimatological studies have revealed past climate dynamics of the northwestern forests in United States (Hessburg et al., 2005), boreal forests in Yukon Territory, Canada (Zalatan and Gajewski, 2005), dry forests in Mongolia (Jacoby et al., 1996; Davi et al., 2006), and Japanese montane forests (Takahashi et al., 2003), to name a few. Tree ring records are especially important data for remote areas where historical records of climate and forest dynamics are largely absent. Moreover, dendrochronological techniques are widely used to study patterns in tree growth and timber production under forest management, such as selective cutting and forest thinning (Bebber et al., 2004; Thorpe et al., 2007).

Radial growth of a tree is simultaneously affected by various environmental constraints; not only by regional factors such as climate fluctuations and large-scale disturbances, but also by local, gap-scale dynamics such as competition and stochastic mortality of neighbor trees (Tessier et al., 1997). Regional climatic factors are,

* Corresponding author. Present address: Frontier Research Center for Global Change, Japan Agency for Marine-Earth Science and Technology, 3173-25 Showa-machi, Kanazawa-ku, Yokohama, Kanagawa 236-0001, Japan.
Tel.: +81 45 778 5595; fax: +81 45 778 5706.
E-mail address: ise@jamstec.go.jp (T. Ise).

0378-1127/$ – see front matter © 2008 Elsevier B.V. All rights reserved.
doi:10.1016/j.foreco.2008.04.007

in general, emphasized in areas where climate strongly limits tree productivity. For example, tree ring variation originating from precipitation trends is especially stressed in relatively arid zones, where the water availability driven by regional climate primarily limits tree growth. Regional patterns in tree rings are relatively homogeneous for these areas, and, among spatially isolated trees in arid zones, local dynamics originating from ecological interactions are not usually dominant (Fritts and Swetnam, 1989). However, in closed-canopy forests, local, gap-scale factors such as competition among neighboring trees are important determinants of tree growth, in addition to the regional factors. For example, canopy closures significantly reduce radial growth (suppression), and non stand-replacing disturbance and selective logging can stimulate growth of surviving trees (release; Black and Abrams, 2003; Druckenbrod, 2005; Thorpe et al., 2007). In many dendrochronological studies, these gap-scale signals were often considered as extraneous variables and filtered out to study regional factors (Fritts and Swetnam, 1989), but from an ecological perspective, such data can provide valuable information about stand history.

There are some previous dendrochronological studies specifically concerning local ecological dynamics. Based on Lorimer and Frelich (1989), Abrams et al. (1995) detected major release events that were defined by a >100% increase in the 15-year average after the year of interest, compared to the average before that year. Similar criteria have been used in other studies (Orwig and Abrams, 1995; Nowacki and Abrams, 1997; Copenheaver and Abrams, 2003). Although moving averages can be sensitive to window size (Kenney and Keeping, 1962), selection of window size in those studies was often arbitrary (*see* Abrams et al., 1995; Nowacki and Abrams, 1997; Copenheaver and Abrams, 2003). In addition, techniques of time-series analysis, such as the Box-Jenkins intervention detection, have been applied to dendrochronological data to estimate the timing of shift in trends (Monserud, 1986; Druckenbrod, 2005).

Local factors such as release, suppression, recovery from disturbance, tend to have persistence in medium-term frequencies (several years to a few decades). Medium-frequency dynamics in tree rings are also affected by large-scale factors such as regional outbreak of insects and pathogens (Berryman et al., 1987), sunspot and solar luminosity cycles (Sonett and Suess, 1984; Willson and Hudson, 1988; Rigozo et al., 2002), El Niño Southern Oscillation (Swetnam and Betancourt, 1990; Villalba et al., 1998), Pacific Decadal Oscillation (D'Arrigo et al., 2001), and North Atlantic Oscillation (Meko et al., 1985). Since those regional signals often have similar timescales of local ecological signals, these two categories of effects are usually difficult to separate (Tessier et al., 1997).

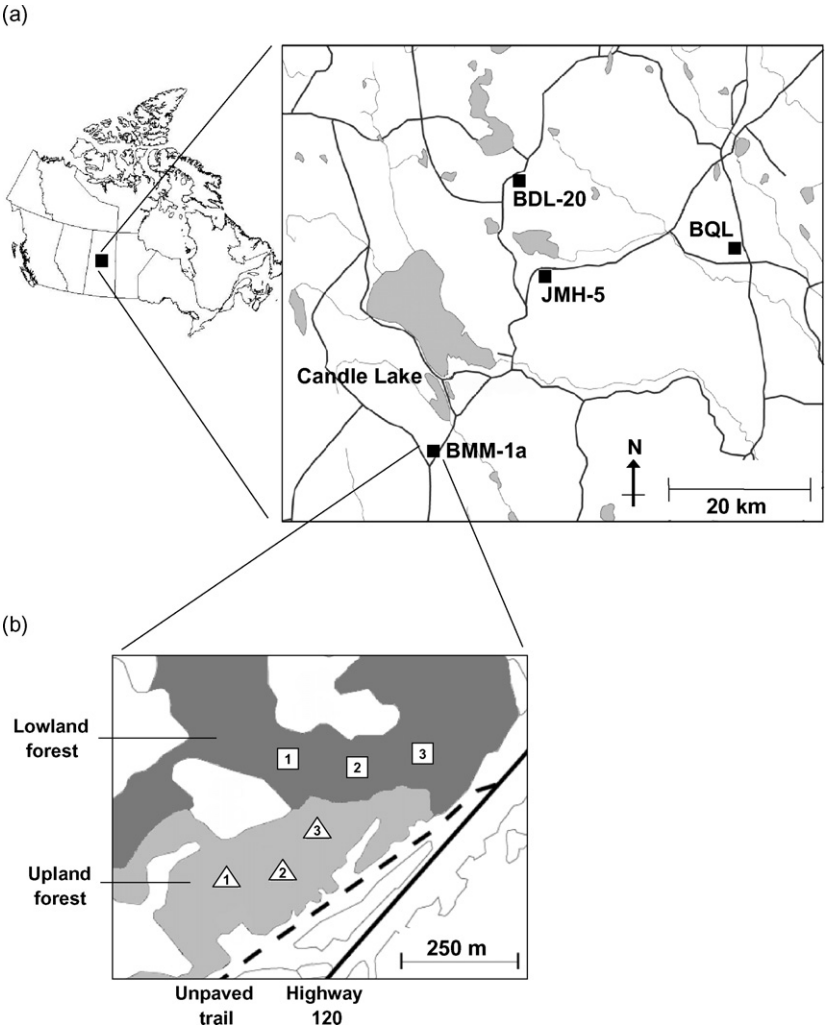

Fig. 1. (a) Location of study sites in the Boreal Ecosystem-Atmosphere Study (BOREAS) Southern Study Area (SSA), Saskatchewan, Canada. Major roads (dark gray) and rivers (light gray) are also shown. (b) Close-up showing site BMM-1a. 3 sampling plots are established in both upland and lowland black spruce stands.

Table 1
Description of study sites in central Saskatchewan, Canada

Site	Drainage	Basal area (m^2 ha^{-1})	Core age (years)
BMM-1a	Upland	23.0	116.9
	Lowland	12.2	76.2
BQL	Upland	25.3	75.1
	Lowland	12.2	101.9
BDL-20	Upland	32.9	110.4
	Lowland	16.1	72.1
JMH-5	Upland	26.0	81.1
	Lowland	12.1	105.2

Upland stands were relatively mature mesic black spruce forests on mineral soils. Lowland stands were poorly drained black spruce woodlands on organic soils. Core ages are conservative estimates of tree ages as not all the samples were cored to the pith or datable to the pith.

In this study, we quantified the relative importance of gap-scale local effects on tree rings with stratified sampling design. First, medium-frequency signals were extracted with an index derived from exponentially weighted moving average (EWMA) in a continuous time series. Then, by using this index, local effects were quantified with an analysis of synchronicity in patterns. Our assumptions were that regional factors such as climatic variations are relatively homogeneous within the given stand, whereas local factors such as stochastic disturbance and competition occur in a less synchronous fashion in a mature stand (Tessier et al., 1997). In a Canadian continental boreal region, we compared synchronicity of medium-frequency tree ring patterns of open- and closed-canopy black spruce (*Picea mariana* (Mill.) B.S.P.) stands, and considered underlying mechanisms of spatial synchronicity.

2. Methods

2.1. Study area and sampling design

We obtained black spruce increment cores from the Southern Study Area (SSA) of the Boreal Ecosystem and Atmosphere Study (BOREAS; Sellers et al., 1995). Black spruce is one of the major forest species in this region (Apps and Halliwell, 1999) and regularly harvested for pulp and fiber production (Geng et al., 2006). Due to the geomorphology shaped by glaciers and ice sheets in the Pleistocene and occasional stand-replacing fires, the landscape is a mosaic of relatively well-drained upland forests and poorly drained woodlands in various ages. Using BOREAS TE-13 site description maps (Apps and Halliwell, 1999), we established 4 sampling sites at least 10 km apart (Fig. 1a). For each site, we selected relatively mature black spruce stands of two drainage types (upland and lowland) in pairs within 500 m (Fig. 1b; Table 1), following the stand map provided by BOREAS TE-13. Based on field and aerial photographs, we assume that the stand map is sufficiently accurate because stand boundaries in this region are often distinctive. In each stand, we established 3 plots ca. 100 m apart using GPS coordinates in advance to ensure randomness of plot selection within stands. We sampled 10 dominant and/or co-dominant black spruce trees closest to the center of each plot. Thus, samples were taken from a roughly circular area centered at each plot coordinates with various area sizes.

In total, 240 black spruce increment cores (4 sites × 2 drainage types × 3 plots × 10 individuals) were taken. Cores were treated with the standard dendrochronological procedures (Fritts, 1976; Cook and Kairiukstis, 1990) in which the cores were glued on mounting wood and surfaced with progressively finer sand papers. Digitally scanned images (2000 dpi) of cores were used for measurement of annual increments using ImageJ 1.36b (Abramoff et al., 2004) with the algorithm of Dendroscan (Varem-Sanders and Campbell, 1996) implemented on R version 2.4.1 (R Development Core Team, 2005). Since 9 cores were severely rotten or had missing fragments, data from 231 increment cores were used for the following analyses.

2.2. Obtaining medium-frequency signals

Although the selection of window size can affect moving averages significantly, previous dendroecological studies often arbitrarily selected the window sizes (e.g., Abrams et al., 1995; Nowacki and Abrams, 1997; Copenheaver and Abrams, 2003). To reduce the sensitivity of the window size due to the abrupt cutoff in simple moving averages, the exponentially weighted moving average (EWMA) was used in this study. To calculate a moving average for a particular point in time, EWMA assigns heavier weights to proximal data points and successively smaller weights to distant data points. EWMA is useful for detecting shifts in the mean of a process (Lucas and Saccucci, 1990) and timing of special causes of variation enter into a system (Lowry et al., 1992). EWMA has been commonly used in economic analyses such as stock price trends (e.g., Domangue and Patch, 1991; Kuen and Hoong, 1992). Like trends in economics, trends in tree rings often occur in various wavelengths, depending on severity and persistence of the impact. Calculation of EWMA after a target year t is:

$$A_t = \frac{\sum_{i=t+1}^{t+c} e^{-\alpha(i-t)} X_i}{\sum_{i=t+1}^{t+c} e^{-\alpha(i-t)}} \quad (1)$$

where X_i is the ring width at year i and α is the extinction coefficient. Although EWMA is an infinite sum in theory, smaller terms were omitted for computational efficiency. The window cutoff size c was set to the year when the sum of weight becomes

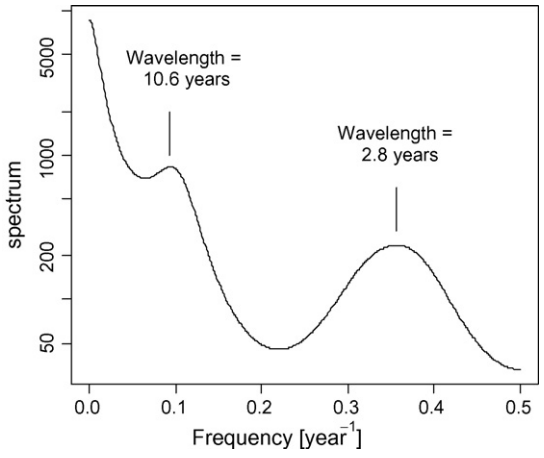

Fig. 2. An example of power spectral analysis (site JMH-5, upland stand, tree number 4). This tree had 2 peaks in medium-frequency trends.

>99% of theoretical total weight. Similarly, calculation of EWMA preceding to a target year t is:

$$B_t = \frac{\sum_{i=t+1}^{t+c} e^{-\alpha(i-t)} X_{2t-i}}{\sum_{i=t+1}^{t+c} e^{-\alpha(i-t)}} \quad (2)$$

Then, following Lorimer and Frelich (1989), a relative change in EWMA after the target year (A_t) compared to EWMA preceding to the target year (B_t) were calculated:

$$\mathrm{SDI}_t = \frac{A_t - B_t}{B_t} \quad (3)$$

This index, stand dynamic index (SDI) is a continuous index that estimates timings of changes in forest dynamics such as release and suppression. When SDI_t is greater than 0, the tree ring pattern in medium-term frequencies at year t has a trend of increase or *vice versa*. Similar to the index based on simple moving average that has one parameter (window size), SDI also has only one parameter (extinction coefficient α).

To determine α objectively, tree ring data from individual trees were analyzed by the power spectral analysis with R version 2.4.1, and peaks in power spectral densities were located (Fig. 2). Then, all peaks found were summarized by the kernel density estimation to find modal wavelengths in medium-frequency trends (Fig. 3). We found 2 distinct peaks at 2.95 and 10.8 years. Thus, to optimally emphasize trends in these wavelengths, 2 values of α were assigned to locate the peaks at the center of gravity of the total theoretical weights (Table 2). Consistencies between different α's were discussed (*see* Section 3).

2.3. Quantifying synchronicity

For each drainage types, patterns of SDI synchronicity within plots and across plots were compared using the two-way repeated measures ANOVA (Wigley et al., 1984; Gotelli and Ellison, 2004):

$$\mathrm{GR}_{ijk} = \mu + \mathrm{PL}_i + \mathrm{TR}_{j(i)} + \mathrm{YR}_k + \mathrm{PL}\cdot\mathrm{YR}_{ik} + \mathrm{YR}\cdot\mathrm{TR}_{kj(i)} \quad (4)$$

In this model for annual growth rings (GR), there were $i = 3$ plots (PL) as a treatment, j individual trees (TR) nested within treatments, and k years of dendrochronological records (YR). TR is the across-individual factor, and YR is the within-individual factor. Across-plot synchronicity is quantified by the treatment effect of PL. When stochastic, gap-scale dynamics dominate the medium-frequency trends, trees in different plots should not be synchronized and variances in the dendrochronological record are largely explained by PL. Conversely, when regionally homogeneous factors dominate the trends, trees in different plots should be synchronized and the fraction of variances explained by PL becomes small, compared with within-plot variation in the residual. We applied the ANOVA for each drainage type for each site (2 drainage types × 4 sites). To quantify the relative importance of plot difference, proportion of explained variance (PEV; η^2 in Jaccard and Guilamo-Ramos, 2002) was calculated:

$$\mathrm{PEV} = \frac{\mathrm{SS_{PL}}}{\mathrm{SS_{PL}} + \mathrm{SS_{RES}}} \quad (5)$$

$\mathrm{SS_{PL}}$ is the sum of squares explained by PL, and $\mathrm{SS_{RES}}$ is the residual sum of squares within plots from the ANOVA (Eq. (4)). PEV quantifies local effects on tree ring trends in medium-term frequencies.

2.4. Validations

Druckenbrod (2005) applied the Box-Jenkins intervention method to estimate timings of release and suppression, using a publicly available tree ring database for the northeastern United States by the FORAST project (McLaughlin et al., 1986). The hurricane of 1938 had a significant impact on forests in the northeastern U.S. and opened canopies by windthrow. The release caused by the hurricane on surviving trees and the

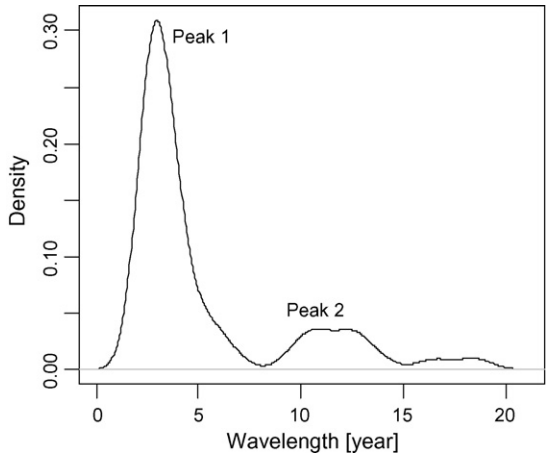

Fig. 3. Kernel density estimation of spectral peaks identified by power spectral analysis. The peak at medium-high frequencies had a modal wavelength of 2.95 years, and for medium-low frequencies, the modal wavelength was 10.8 years.

Table 2
Set of extinction coefficients (α) used for exponentially weighted moving average (EWMA) and characteristic timescale for each α

Extinction coefficient (α)	Y_{50}	c
0.35	2.95	14
0.071	10.8	36

Y_{50} is the year at the center of gravity of the weight where 50% of the total weight is included. The window cutoff size c is the number of years where 99% of the total weight is included, and calculation of EWMA was terminated at c and smaller terms were omitted.

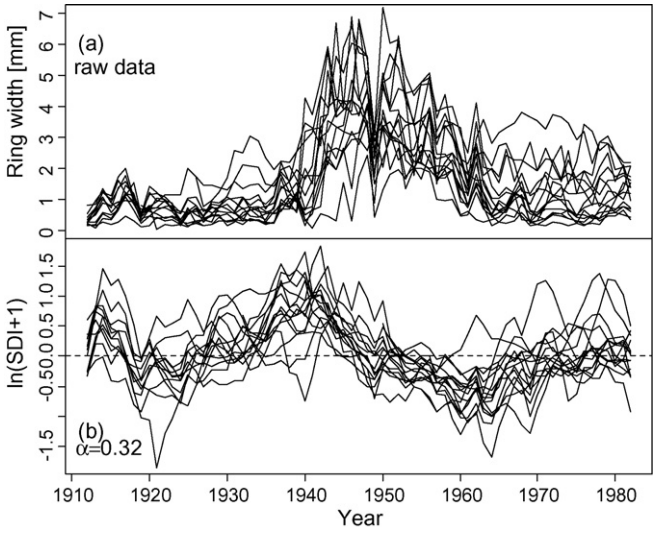

Fig. 4. (a) Raw tree ring time series and (b) stand dynamic index (SDI) calculated from exponentially weighted moving average (EWMA), for 15 eastern hemlock cores in Site 7 of FORAST Database (McLaughlin et al., 1986). SDI, an estimate of timing of forest dynamics change, was high around 1938, indicating the hurricane of 1938 was a significant factor to change forest dynamics, by opening the forest by windthrow (release). Similarly, SDI estimated timing of canopy closure in 1950s and 1960s. The extinction coefficient (α = 0.32) was determined by the power spectral analysis and the kernel density estimation.

following suppression due to canopy closure was observed in the annual increment data in the FORAST database. With the same data of 15 eastern hemlock (*Tsuga canadensis*) cores from New Hampshire, USA, we calculated SDI and compared detected release and suppression timings with Druckenbrod (2005). This validation on tree ring data with known forest history evaluates the ability of SDI to provide a record of forest dynamics, although it remains uncertain that the result from northern temperate hemlock can directly be applicable to boreal black spruce stands.

3. Results

Using exponentially weighted moving averages (EWMA), we calculated SDI to estimate timings of events in radial growth time series, in medium-term frequencies. First, to evaluate the ability of SDI to capture medium-frequency trends, we calculated SDI for 15 eastern hemlock cores from New Hampshire, USA in FORAST Database (McLaughlin et al., 1986) and studied timings of release and suppression events detected in SDI (Fig. 4). Changes in forest dynamics were occurring near the 1938, indicating the hurricane

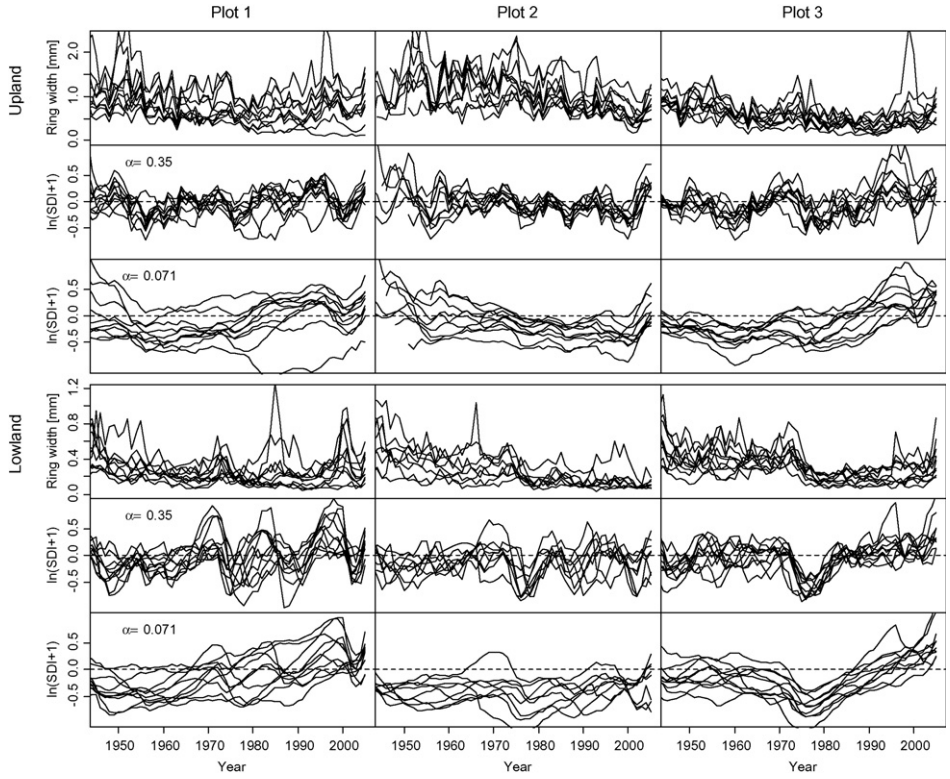

Fig. 5. Raw tree ring data and SDI in site JMH-5. Trees in plot 3 of the lowland stand showed high synchronicity compared to other plots ($p < 0.001$), and thus the effect of plot was significant in lowland stand.

Table 3
Comparison of proportion of variance explained by plot (PEV; Eq. (5))

Site	Drainage	α	PEV	p-value
BMM-1a	Upland	0.35	0.204	0.055 *
		0.071	0.226	0.039 **
	Lowland	0.35	0.061	0.484
		0.071	0.089	0.342
BQL	Upland	0.35	0.271	0.013 **
		0.071	0.354	0.002 ***
	Lowland	0.35	0.102	0.232
		0.071	0.095	0.256
BDL-20	Upland	0.35	0.219	0.035 **
		0.071	0.129	0.153
	Lowland	0.35	0.014	0.832
		0.071	0.079	0.325
JMH-5	Upland	0.35	0.129	0.165
		0.071	0.079	0.340
	Lowland	0.35	0.451	<0.01 ***
		0.071	0.378	<0.01 ***

ANOVA (Eq. (4)) was carried out separately for 4 sites, 2 drainage types, and 2 extinction coefficients (α).
*$p < 0.1$; **$p < 0.05$; ***$p < 0.01$.

of 1938 had a large impact on forest dynamics by opening the canopy by windthrow (release; Foster et al., 1998). Similarly, SDI detected timings of canopy closure (suppression) in 1950s and 1960s, consistent with Druckenbrod (2005). Note that peaks in SDI did not correspond to those in raw data because ring widths usually reached maxima with time lags after the event.

The raw increment data from BOREAS SSA were then individually converted to SDI (Fig. 5). Synchronicity of SDI among plots was analyzed by two-way repeated measures ANOVA (Gotelli and Ellison, 2004). We applied the ANOVA for upland and lowland stands separately, and the synchronicity from 2 stands was compared (Table 3). PEV was larger for upland stands than lowland stands except JMH-5. Since upland stands had larger basal area than lowland stands (Table 1) and closed canopies, local dynamics such as competition were, in general, more pronounced. To accommodate medium-frequency trends in 2 distinct wavelengths, we used 2 extinction coefficients found in spectral density analysis (Table 2). Results with different α's were generally consistent, suggesting medium-frequency trends in modal wavelengths of 2.95 and 10.8 years were affected by local factors in a similar proportion. For BDL-20, we found a significant effect of plot with $\alpha = 0.35$ ($p = 0.035$) but not with $\alpha = 0.071$ ($p = 0.153$). This suggested that heterogeneity among plots was strong around the wavelength of 2.95 years, compared to that around 10.8 years. The effect of stand ages (Table 1) on SDI was not significant ($p = 0.25$).

Site JMH-5 had a unique pattern (Fig. 5; Table 3). PEV for the lowland stand was high (0.320–0.398) and highly significant ($p < 0.001$). This was possibly because all trees in plot 3 in the lowland stand of JMH-5 were concentrated on a narrow sand bar within a continental bog, and thus tree ring patterns were highly synchronized compared to other plots ($p < 0.001$). It is likely that this anomalous plot increased within-plot synchronicity and reduced across-plot synchronicity.

To test the significance of SDI, we calculated PEV directly from the raw data and compared to SDI-based PEV (Fig. 6). If SDI captured a similar trend of the raw data, the two indices (raw data- and SDI-based PEVs) are likely to have a 1-to-1 relationship. The absence of such a relationship indicated that the synchronicity in SDI were distinct from that in the raw data. Filtering high-frequency signals, SDI thus successfully captured unique dynamics in medium-term frequencies, and the underlying mechanisms of medium-frequency trends were different from those of high-frequency trends. The correlation coefficient between SDI-based and raw data-based PEV was marginally negative ($r = -0.44$; $p = 0.09$), implying that plots with high synchronicity in medium-term frequency tend to have low synchronicity in high frequency.

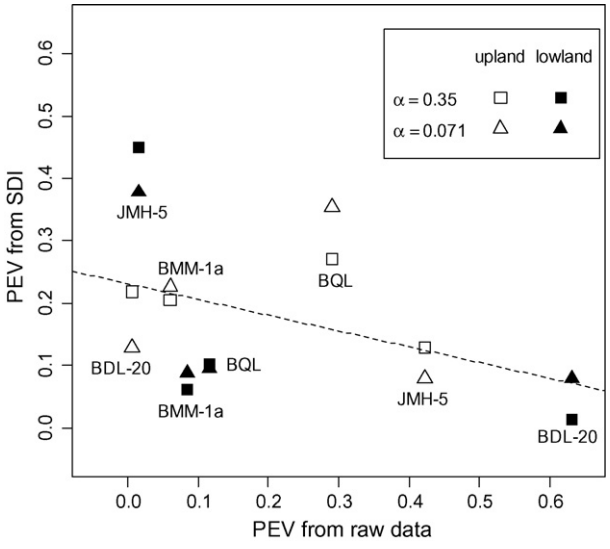

Fig. 6. Comparison between SDI-based PEV against raw data-based PEV (open symbols: upland plots; filled symbols: lowland plots; *square*: $\alpha = 0.35$; triangle: $\alpha = 0.071$). The linear regression line is also shown ($r = -0.44$; $p = 0.09$).

4. Discussion

Our results were generally consistent with the conventional observations in dendrochronology; in closed, high-density forests, local forest dynamics often played a significant role in medium-frequency patterns in tree rings (PEV: 12.9–35.4%, except JMH-5). This result implies that dendroclimatological studies in closed-canopy forests should appropriately treat trends from local effects to identify regional patterns. For the upland stand in BDL-20, a significant effect of plot-level heterogeneity was found in medium-high frequencies ($\alpha = 0.35$) but not in medium-low frequencies ($\alpha = 0.071$). For this relatively mature dense stand, it is possible that disturbances of low persistence (e.g., minor damage) were stochastic, and that major disturbances, such as tree mortality, were evenly dispersed throughout the forest.

In lowland, open woodlands, except JMH-5, effects from local dynamics were not statistically detected, indicating that local factors such as gap dynamics were not the major determinants of tree ring patterns in medium-term frequencies (PEV: 1.4–10.2%, except JMH-5). The unique pattern of JMH-5 can be explained by local conditions. Since all of 10 trees in the plot 3 of the wet site were on a narrow sand bar, the trees had highly synchronized SDI patterns, compared to other trees in the same continental bog. It is likely that local dynamics such as changes in hydrology simultaneously affected the trees and caused this synchronicity. On the other hand, due to high heterogeneity in boreal peatland hydrology (Camill and Clark, 2000), this pattern was not duplicated for the other plots in the same stand.

To consider an alternative explanation of the pattern of synchronicity, we statistically evaluated possible effects of stand age on this study, using core age (Table 1) as an estimation of stand age. There was no difference between mean core ages among upland and lowland stands ($p = 0.62$, mean core ages were 96 and 89 years, respectively). The effects of core age on PEV were also absent ($p = 0.23$ for upland and $p = 0.59$ for lowland stands), within the range of core ages in this study (72–117 years). However, an influence from stand age can be significant if PEV is analyzed on stands with wider ages. We also verified the biometric homogeneity of stands by analyzing the correlation between within-stand variations of basal area and PEV. Since there was no effect of basal area on PEV ($p = 0.79$), the variation in synchronicity is not likely the result of inappropriate delineation of stands.

In conclusion, we separated regional-scale dynamics (e.g., climatic variation and large-scale insect outbreak) and local dynamics (e.g., forest gap dynamics and local hydrological change) in medium-term frequencies and quantified the relative contributions from local factors in tree ring trends. The medium-frequency trends are characteristic to the ecological signals and significantly different from high-frequency interannual trends (Fig. 6). These advancements in statistical analysis and study design will help both ecologists and paleo-climatologists to objectively evaluate the effects from climate fluctuations, relative to the effects from local, ecological interactions. Moreover, detection and quantification of release caused by forest management practices such as selective cutting (Bebber et al., 2004; Thorpe et al., 2007) is a major application of this study. By constructing and analyzing SDI, timing, magnitude, and duration of release found in the medium-frequency signals can be studied.

Acknowledgements

We greatly appreciate helpful discussions with Profs. Thomas W. Swetnam and Konrad Gajewski and Dr. David A. Orwig. We thank Dr. Allison L. Dunn and Yuko Hasegawa for help on field study design and sampling. The graduate study of Takeshi Ise was supported by the James Mills Peirce Fellowship provided by the Department of Organismic and Evolutionary Biology at Harvard University.

References

Abramoff, M.D., Magelhaes, P.J., Ram, S.J., 2004. Image processing with ImageJ. Biophotonics International 11, 36–42.
Abrams, M.D., Orwig, D.A., Demeo, T.E., 1995. Dendroecological analysis of successional dynamics for a presettlement-origin white-pine mixed-oak forest in the Southern Appalachians, USA. Journal of Ecology 83, 123–133.
Apps, M.J., Halliwell, D., 1999. BOREAS TE-13 biometry reports. Data set. Available on-line [http://www.daac.ornl.gov] from Oak Ridge National Laboratory Distributed Active Archive Center, Oak Ridge, Tennessee, U.S.A.
Bebber, D.P., Thomas, S.C., Cole, W.G., Balsillie, D., 2004. Diameter increment in mature eastern white pine *Pinus strobus* L. following partial harvest of old-growth stands in Ontario, Canada. Trees-Structure and Function 18, 29–34.
Berryman, A.A., Stenseth, N.C., Isaev, A.S., 1987. Natural regulation of herbivorous forest insect populations. Oecologia 71, 174–184.
Black, B.A., Abrams, M.D., 2003. Use of boundary-line growth patterns as a basis for dendroecological release criteria. Ecological Applications 13, 1733–1749.
Camill, P., Clark, J.S., 2000. Long-term perspectives on lagged ecosystem responses to climate change: permafrost in boreal peatlands and the grassland/woodland boundary. Ecosystems 3, 534–544.
Cook, E.R., Kairiukstis, L.A., 1990. Methods of Dendrochronology. Kluwer, Boston.
Copenheaver, C.A., Abrams, M.D., 2003. Dendroecology in young stands: case studies from jack pine in northern lower Michigan. Forest Ecology and Management 182, 247–257.
D'Arrigo, R., Villalba, R., Wiles, G., 2001. Tree-ring estimates of Pacific decadal climate variability. Climate Dynamics 18, 219–224.
Davi, N.K., Jacoby, G.C., Curtis, A.E., Baatarbileg, N., 2006. Extension of drought records for central Asia using tree rings: West-central Mongolia. Journal of Climate 19, 288–299.
Domangue, R., Patch, S.C., 1991. Some omnibus exponentially weighted moving average statistical process monitoring schemes. Technometrics 33, 299–313.
Druckenbrod, D.L., 2005. Dendroecological reconstructions of forest disturbance history using time-series analysis with intervention detection. Canadian Journal of Forest Research 35, 868–876.
Foster, D.R., Knight, D.H., Franklin, J.F., 1998. Landscape patterns and legacies resulting from large, infrequent forest disturbances. Ecosystems 1, 497–510.
Fritts, H.C., 1976. Tree Rings and Climate. Academic Press, London.
Fritts, H.C., Swetnam, T.W., 1989. Dendroecology—a tool for evaluating variations in past and present forest environments. Advances in Ecological Research 19, 111–188.
Geng, X.L., Zhang, S.Y., Deng, J., 2006. Alkaline treatment of black spruce bark for the manufacture of binderless fiberboard. Journal of Wood Chemistry and Technology 26, 313–324.
Gotelli, N.J., Ellison, A.M., 2004. A Primer of Ecological Statistics. Sinauer, Sunderland, MA.
Hessburg, P.F., Kuhlmann, E.E., Swetnam, T.W., 2005. Examining the recent climate through the lens of ecology: inferences from temporal pattern analysis. Ecological Applications 15, 440–457.
Jaccard, J., Guilamo-Ramos, V., 2002. Analysis of variance frameworks in clinical child and adolescent psychology: advanced issues and recommendations. Journal of Clinical Child Psychology 31, 278–294.
Jacoby, G.C., Darrigo, R.D., Davaajamts, T., 1996. Mongolian tree rings and 20th-century warming. Science 273, 771–773.
Kenney, J.F., Keeping, E.S., 1962. Mathematics of Statistics, Pt. 1, 3rd ed. Van Nostrand, Princeton.
Kuen, T.Y., Hoong, T.S., 1992. Forecasting volatility in the Singapore stock market. Asia Pacific Journal of Management 9, 1–13.
Lorimer, C.G., Frelich, L.E., 1989. A methodology for estimating canopy disturbance frequency and intensity in dense temperate forests. Canadian Journal of Forest Research 19, 651–663.
Lowry, C.A., Woodall, W.H., Champ, C.W., Rigdon, S.E., 1992. A multivariate exponentially weighted moving average control chart. Technometrics 34, 46–53.
Lucas, J.M., Saccucci, M.S., 1990. Exponentially weighted moving average control schemes: properties and enhancements. Technometrics 32, 1–12.
McLaughlin, S.B., Downing, D.J., Blasing, T.J., Jackson, B.L., Pack, D.J., Duvick, D.N., Mann, L.K., Doyle, T.W., 1986. FORAST database [online]. Carbon Dioxide Information Analysis Center. Available from http://cdiac.ornl.gov/ndps/db1005.html.
Meko, D.M., Stockton, C.W., Blasing, T.J., 1985. Periodicity in tree rings from the Corn Belt. Science 229, 381–384.
Monserud, R.A., 1986. Time-series analyses of tree-ring chronologies. Forest Science 32, 349–372.
Nowacki, G.J., Abrams, M.D., 1997. Radial-growth averaging criteria for reconstructing disturbance histories from presettlement-origin oaks. Ecological Monographs 67, 225–249.
Orwig, D.A., Abrams, M.D., 1995. Dendroecological and ecophysiological analysis of gap environments in mixed-oak understoreys of northern Virginia. Functional Ecology 9, 799–806.
R Development Core Team, 2005. R: A Language and Environment for Statistical Computing. R Foundation for Statistical Computing, Vienna, Austria.
Rigozo, N.R., Nordemann, D.J.R., Echer, E., Zanandrea, A., Gonzalez, W.D., 2002. Solar variability effects studied by tree-ring data wavelet analysis. Advances in Space Research 29, 1985–1988.
Sellers, P., Hall, F., Margolis, H., Kelly, B., Baldocchi, D., Denhartog, G., Cihlar, J., Ryan, M.G., Goodison, B., Crill, P., Ranson, K.J., Lettenmaier, D., Wickland, D.E., 1995. The boreal ecosystem-atmosphere study (BOREAS)—an overview and early results from the 1994 field year. Bulletin of the American Meteorological Society 76, 1549–1577.
Sonett, C.P., Suess, H.E., 1984. Correlation of bristlecone pine ring widths with atmospheric C-14 variations—a climate sun relation. Nature 307, 141–143.
Swetnam, T.W., Betancourt, J.L., 1990. Fire-Southern Oscillation relations in the southwestern United States. Science 249, 1017–1020.
Takahashi, K., Azuma, H., Yasue, K., 2003. Effects of climate on the radial growth of tree species in the upper and lower distribution limits of an altitudinal ecotone on Mount Norikura, central Japan. Ecological Research 18, 549–558.
Tessier, L., Guibal, F., Schweingruber, F.H., 1997. Research strategies in dendroecology and dendroclimatology in mountain environments. Climatic Change 36, 499–517.
Thorpe, H.C., Thomas, S.C., Caspersen, J.P., 2007. Residual-tree growth responses to partial stand harvest in the black spruce (*Picea mariana*) boreal forest. Canadian Journal of Forest Research 37, 1563–1571.
Varem-Sanders, T.M.L., Campbell, I.D., 1996. Dendroscan: A Tree-ring Width and Density Measurement System. Canadian Forest Service Northern Forestry Centre, UBC Press, Vancouver.
Villalba, R., Cook, E.R., Jacoby, G.C., D'Arrigo, R.D., Veblen, T.T., Jones, P.D., 1998. Tree-ring based reconstructions of northern Patagonia precipitation since AD 1600. Holocene 8, 659–674.
Wigley, T.M.L., Briffa, K.R., Jones, P.D., 1984. On the average value of correlated time-series, with applications in dendroclimatology and hydrometeorology. Journal of Climate and Applied Meteorology 23, 201–213.
Willson, R.C., Hudson, H.S., 1988. Solar luminosity variations in solar cycle-21. Nature 332, 810–812.
Zalatan, R., Gajewski, K., 2005. Tree-ring analysis of five *Picea glauca* dominated sites from the Interior boreal forest in the Shakwak Trench, Yukon Territory, Canada. Polar Geography 29, 1–16.